Nano Research

Open Access

Research Article

Naturphilosophie unfolding in bacterial microcolony revealed by global single-cell/fluid-nanotracer tracking

Yuqian Sang, Qian Ren, Ziyang Zhang, Yongyu Zhang, and Yan He ✉

Department of Chemistry, Key Laboratory of Bioorganic Phosphorus Chemistry & Chemical Biology (Ministry of Education), Tsinghua University, Beijing 100084, China

Cite this article: *Nano Research*, **2026**, *19*, 94908449. https://doi.org/10.26599/NR.2026.94908449

ABSTRACT: Nature, viewed philosophically, is an inherent principle of self-constitution and dynamic unfolding. Here, we explore these profound principles not by contemplating the vastness of the cosmos, but within the confines of *Bacillus subtilis* microcolony—a tractable micro-*Entity* where individual-collective interplay becomes observable under a microscope. By tracking the complete spatiotemporal evolution at single-cell/particle resolution, we reveal multi-stage self-organization driven by sequential evolutionary pressures (environmental, peer, differentiation, boundary), manifesting the essential dynamism of the active fluid medium (*Copula*) that co-evolves with individual bacterial behaviors. In the sparse earliest stage, initial environmental constraints amplify subtle individual variations, triggering a behavioral bifurcation (near-linear traversal vs. large-radius circulation). As cell density increases, heterogeneous intercellular structures emerge, including a dynamic partitioning of "motile" and "static" regions. Notably, even in the highly crowded late stage, a large population of bacteria maintain superdiffusion rather than dynamical arrest. Synchronous tracking of passive fluid nanotracers (~ 200 nm oil-droplets) demonstrates how bacterial activity generates intercellular fluid field and transforms near-Brownian transport into superdiffusive flows, unveiling collective coordination mediated by the bacterial *Copula*. This comprehensive picture of multi-step dynamic transitions establishes bacterial microcolony evolution as a compelling model system for deciphering the emergence of forms and functions in a living micro-*Entity*, bridging scientific and philosophical perspectives.

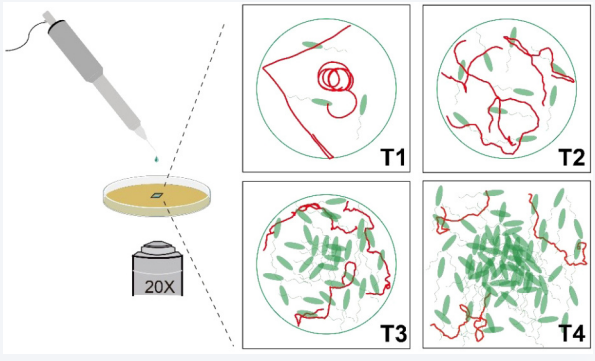

KEYWORDS: bacterial collective evolution, single-cell tracking, single-nanoparticle tracking, superdiffusion, bacteria-fluid coupling

1 Introduction

The fundamental inquiry into the dynamic emergence of order, particularly the relationship between individuals and the whole and the progressive differentiation of complex systems, has animated natural philosophy since its inception [1]. For over two millennia until the early 1800s, thinkers from Plato to Schelling grappled with these questions primarily through philosophical reflection, as contemporary experimental tools available afforded only coarse-grained observations of natural phenomena [2]. Their conception of *Natura naturans*, a self-constituting principle driving the emergence of the observable world (*Natura naturata*) through a dynamic *Copula* mediating potentiality and actualized manifestations, established a profound framework for understanding nature's inherent creativity [3]. Yet phenomena such as the self-organized evolution of biological collectives, where microscopic interactions give rise to macroscopic order, could not even be imagined through abstract reasoning [4]. Today, driven by revolutionary advancements in microscopy and imaging techniques, we possess unprecedented capabilities to observe the intricacies of natural processes at high resolution. This technological leap allows us to transcend philosophical speculation and empirically investigate fundamental questions of self-organization and individual-whole relationship in living systems. As model *Organismus*, microbial communities offer ideal testbeds for such empirical inquiry.

From the synchronized flight of schools of birds [5] to the coordinated migration of cells [6], the living world is abundant with examples of collective behaviors, where interactions between

Received: November 23, 2025; **Revised:** January 15, 2026
Accepted: January 15, 2026

✉Address correspondence to yanhe2021@mail.tsinghua.edu.cn

individuals give rise to macroscopic order and function that transcend individual capabilities [7]. At the microbial level, bacteria also exhibit highly sophisticated collective coordination [8]. By sensing and responding to environmental cues through direct physical contact, chemical signaling (e.g. quorum sensing) and hydrodynamic coupling [9–11], they progressively organize into "superorganisms" including biofilms, microcolonies, and swarming arrays [12–15]. These collective structures are critical adaptive strategies for bacteria to survive in diverse environments, resist external stresses such as antibiotics, and use resources efficiently through coordinated metabolism [16–18]. Unlike complex organisms with conscious motivations, the underlying drive for bacteria is a fundamental biological imperative: the instinct to survive and thrive [19]. This intrinsic biological *Wollen* in Schelling's ontological sense as primal striving-to-be manifests as the relentless pursuit of resources, growth, adaptation, and propagation. It constitutes the dynamic principle that drives their individual actions and, collectively, the self-unfolding of the living system. The process of their formation and evolution—from dispersed individual cells to structured populations—embodies profound principles of non-equilibrium physics and collective ecology [20]. Understanding this complete evolutionary pathway, i.e., how individual behavior driven by the survival imperative drives the emergence of macroscopic structures, and how the collective structure and environment in turn regulate single bacterial behavior, is a central question in microbial ecology [21, 22]. This process reveals how the elemental *Wollen* of individual *Momente* (spatiotemporally dispersed constituents) dynamically constitutes the collective *Entity*, and how the environment acts as a mediating *Copula*, shaping this self-constitution [23].

Despite decades of intensive research using conventional approaches including macroscopic morphological assays (e.g., colony expansion patterns, biofilm thickness measurements) [24, 25], molecular genetics (e.g., signaling pathway analysis, gene expression regulation) [26–29], and theoretical modeling (e.g., particle-based simulations, continuum mechanics) [30–32], a high-resolution picture of the complete evolutionary process of a living bacterial collective, from its sparse initiation to its mature complex architecture, remains elusive. Traditional single-cell tracking, constrained to narrow imaging fields, captures only localized regions (e.g., colony edges or biofilm sections) [33, 34], unable to monitor long-range coordination, competitive dynamics, and system-wide spatiotemporal heterogeneity—precisely the phenomena expressing the *Entity*'s self-constitution and the *Copula*'s mediating function across the entire system. Conversely, macroscopic imaging, though recording global morphology or bulk flow properties, sacrifices single-cell-resolution kinetics (e.g., motion patterns, speed distribution, mobility modulation, interaction events), and cannot establish direct causal links between microscopic mechanisms and macroscopic phenomena [35, 36]. This scale-resolution dichotomy impedes mechanistic understanding of the dynamic transitions and the interplay of driving forces throughout the system's self-constitution. Meanwhile, most theoretical frameworks oversimplify bacterial cells as self-propelled particles in a passive medium, or focus solely on cell–cell interactions, thereby neglecting the fluid environment's active role as a dynamic mediator—the *Copula* that orchestrates collective dynamics, while being co-generated by the active *Momente*.

To bridge this gap, we introduce a unique experimental platform: long-term, wide-field live imaging of the complete evolution of a *Bacillus subtilis* microcolony initiated from a minimal liquid droplet on agar. This system provides a controlled "microcosm" where the entire self-organizing process, driven by cell proliferation and the primal impulse for survival and reproduction, unfolds under the microscope. By simultaneously tracking individual bacteria and passive nanotracers, i.e., probing individual *Momente* of the "active medium" or *Copula*, we elucidate fundamental principles governing the living active matter. Beyond phenomenological description, we decipher how the inherent dynamism and relational logic of the system—fueled by the bacterial imperative—drive its self-unfolding and the emergence of complex form and function. Viewing the evolving microcolony as an empirically accessible manifestation of *Natura naturans*, this approach delivers quantitative evidence for principles once can only be contemplated philosophically, exposing the generative complexity of life's self-constitution.

2 Results

In a typical experiment, we performed long-term continuous observation of the global evolution of a *Bacillus subtilis* microcolony (600–800 μm in diameter) from early settlement to the expansion phase (Movie S1 in the Electronic Supplementary Material (ESM)). We found that as cell proliferation and density increased, the microcolony evolution progressed through different stages of organization, each exhibiting distinct collective behavior patterns arising from the evolving fluid environment and the changing interactions between individual bacterial cells. These stages included: 1) the formation of multilayer bacterial structures from a monolayer distribution, 2) the separation of motile and static regions, and 3) the ultimate breaking of the original boundary. We systematically tracked and analyzed the trajectories of individual bacteria at different time points, obtaining parameters including cell speed and direction distribution, mean square displacement (MSD), anomalous diffusion exponent (α), radius of gyration (Rg), and motion patterns over time. This qualitative and semi-quantitative information provides a detailed picture of the microcolony evolution (Fig. 1).

2.1 Spatiotemporal heterogeneity of microcolony evolution: the emergence of differentiated structure

Initially (< ~ 3 min), the droplet rapidly spreads on the agar surface, resulting in a microcolony of very thin liquid layer and strong interfacial constraints. Of a total of ~ 900 bacteria within the colony boundary, most were quickly confined to the edge, forming a relatively static, high-density ring (Fig. 2(a)). Only a few cells were able to move freely in the central region of the microcolony, exhibiting bacterial motility within the limited space. With the passage of time and rapid increase in cell density, multilayer structures began to develop inside the colony. Cells started to show localized coordinated movements, suggesting the emergence of collective interactions. At ~ 120 min, transient, side-by-side movements of clusters of only 2–3 cells appeared (Fig. 2(b)), representing early, limited forms of collective organization. At ~ 180 min, larger clusters or raft-like collective migration involving dozens of cells emerged (Fig. 2(c)), indicating the amplification of collective effects, likely mediated by hydrodynamic coupling. Between ~ 220–250 min, "phase separation" occurred within the colony, reflecting the dynamic partitioning of the

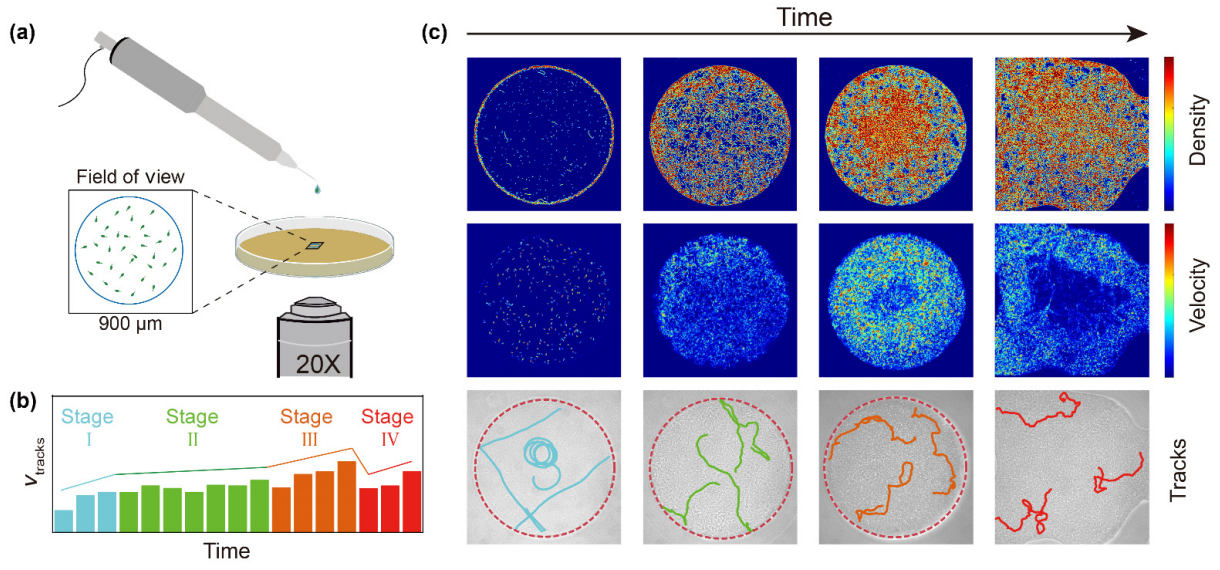

Figure 1 Imaging and analysis of bacterial colony evolution across discrete developmental stages. (a) Schematic illustration of time-resolved observation of a *Bacillus subtilis* colony. A 30 nL droplet of bacterial suspension is inoculated onto an agar surface, forming a microcolony that remains entirely within the field of view under a 20× objective, enabling us to capture its complete journey of self-organization. (b) The microcolony development is segmented into four discrete stages, defined by emergent differences in bacterial motility and color-coded for visualization. (c) Comparative analysis of the microcolony parameters across these stages. The top row, color-coded cell density distribution; the middle row, single-pixel velocity magnitudes; the bottom row, overlay of representative bacterial trajectories on the corresponding raw phase contrast images.

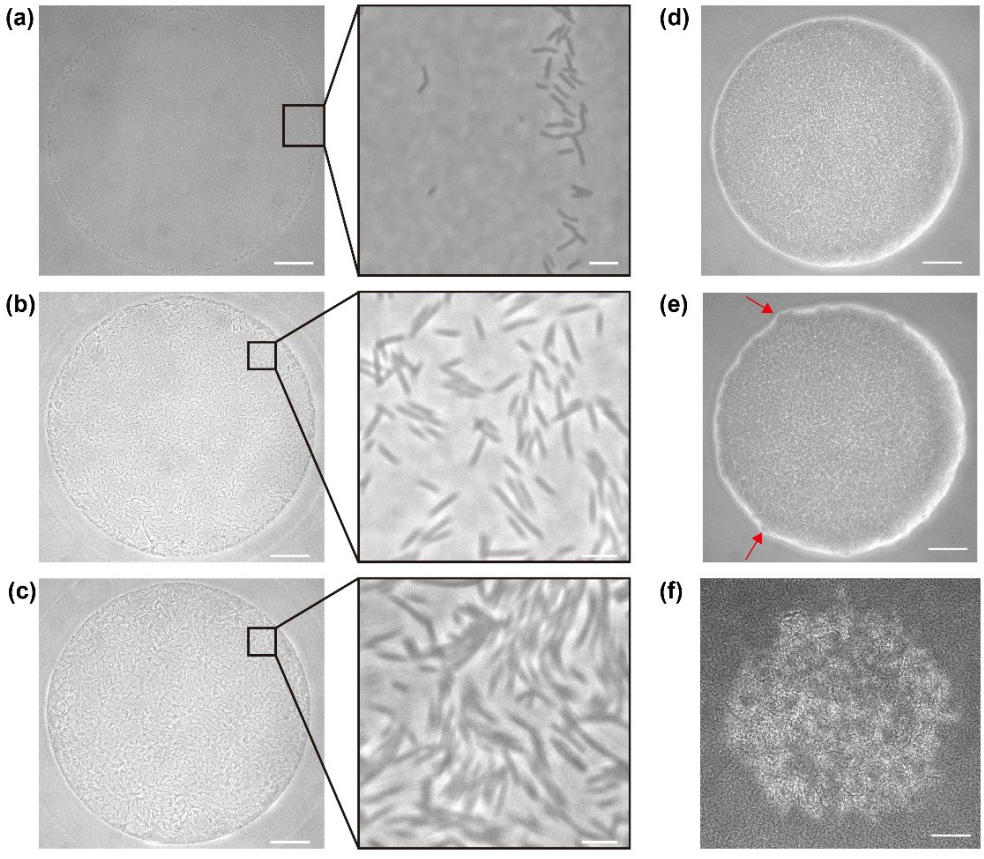

Figure 2 Phase-contrast images of the dynamic formation and restructuring of the bacterial microcolony, demonstrating the spatially heterogeneous nature of its self-constitution. Scale bar is 100 μm unless stated otherwise. (a) At 20 min post-inoculation, initial formation of an ordered microcolony boundary is observed, marking the nascent *Entity*. Overview (left); enlarged view (right, scale bar 10 μm). (b) At 120 min, side-by-side alignment of individual bacteria begins to emerge, indicating the onset of collective interactions within the active medium. Overview (left); enlarged view (right, scale bar 5 μm). (c) By 180 min, the microcolony transitions into a cluster-like organization, showing increased influence of cohesive forces. Overview (left); enlarged view (right, scale bar 5 μm). (d) At 250 min, the overall morphology of the microcolony. (e) At 300 min, peripheral protrusions become evident, indicative of heterogeneous edge expansion. (f) At 340 min, a 3D reticulate architecture emerges within the microcolony.

microcolony into distinct functional regions: slow-moving or stationary bacteria gradually connected with each other to form three-dimensional (3D) irregularly branched or reticulated structures ("stationary domains"); while unconstrained bacteria moved rapidly around or within the gaps of these structures ("motile regions") (Fig. 2(d)). Particle image velocimetry (PIV) analysis of the velocity field also confirmed the transition from an early relatively dispersed low-speed state to a later mixed high- and low-speed state, as well as the intricate changes in the formation, expansion, movement, combination, and splitting of the stationary regions of different sizes and shapes at different locations (Figs. S1 and S2 in the ESM). Rather than showing a uniform pattern with a monotonic density or velocity gradient from the center to the edge of the microcolony, the entire bacterial community exhibited entanglements of different subpopulations with various speeds and thus distinct functional units. At ~ 300 min, the surfactant secreted by the bacteria accumulated into a thin, rapidly diffusing front at the edge of the microcolony, generating additional traction that caused the edge bacteria to break the original geometric boundary, form finger-like protrusions, and begin irregular expansion (Fig. 2(e)). Meanwhile, the central region of the microcolony became dominated by an interconnected 3D cell network, with only a few bacteria moving within the pores of the network (Fig. 2(f)). Consequently, the colony started to exhibit the familiar pattern of high activity at the periphery and relative stasis at the center. These observations clearly demonstrate that the global evolution of the microcolony is a highly dynamic, structurally complex, and spatially heterogeneous self-organizing process—a continuous unfolding of the *Natura naturata*.

2.2 Individual bacterial dynamics under early environmental constraints: the emergence of distinct behavioral patterns

Single-cell trajectory analysis revealed significant, multi-stage dynamic changes in individual bacterial movement patterns (Fig. S3 in the ESM). At the earliest stage of colonization (< 15 min), beyond the edge-confined majority, a few bacteria moving in the central region exhibited two distinct patterns despite being in proximity: Some performed long-range, near-linear traversals, exploring the limited space with directional changes only upon boundary collision; some exhibited stable, large-radius circular motions, persisting in localized rotation for extended periods (Fig. 3(a) and Movie S2 in the ESM). This coexistence of behavioral dimorphism under the same macroscopic environmental pressure suggests that subtle individual differences or stochasticity (possibly related to flagellar bundle conformation, transient interactions with upper air/liquid interface or lower liquid/solid interface, or cellular internal states) are amplified under strong physical constraints (the initial boundary conditions of the active fluid medium), leading to "personalized" selection of movement strategy. This brief window of coexisting extreme behaviors lasted ~ 10 min, after which near-linear and circular motions significantly diminished and the trajectories of most motile bacteria transitioned to the hybrid of linear segments and turns of varying radii (Fig. S4 in the ESM).

Statistical results showed that during the 0–40 min period, the average speed of motile bacteria was initially ~ 26 μm/s, then gradually increased, stabilizing at ~ 43 μm/s after ~ 25 min (Fig. 3(b)). Further analysis revealed a broad velocity distribution in early times, and then the peak narrowed and shifted to higher

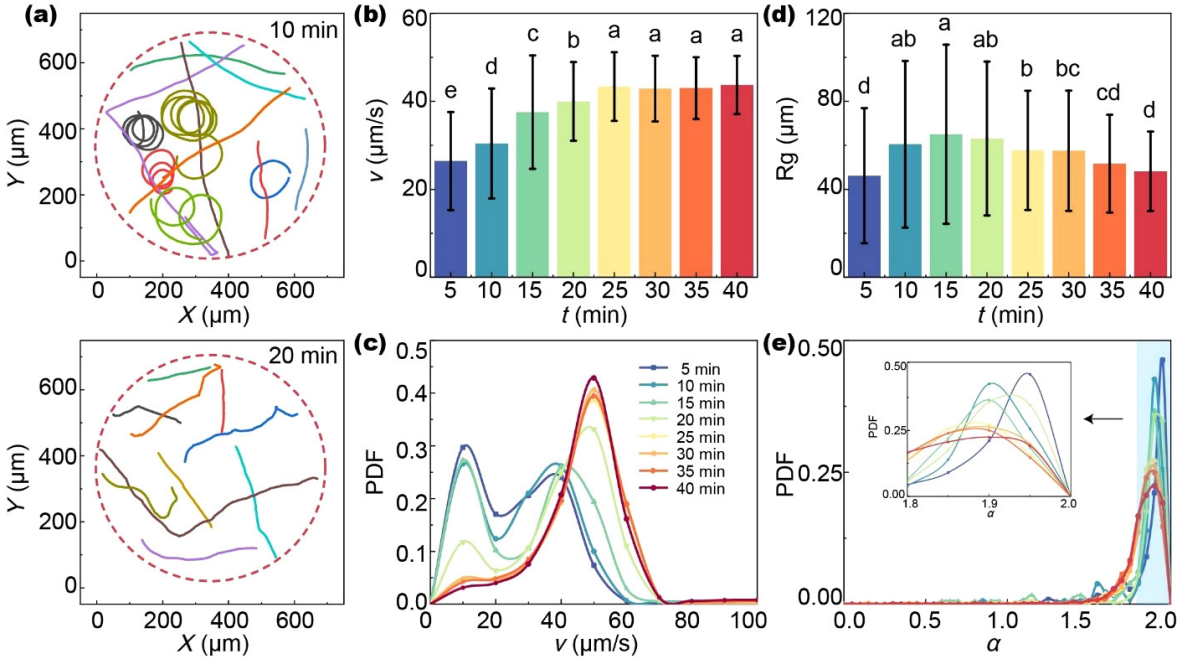

Figure 3 Single-cell trajectories and motility characteristics during early-stage of the microcolony evolution. (a) Representative single-cell trajectories illustrating motility behaviors at early time points. Top: two distinct motility patterns observed at 10 min after inoculation, showing the emergence of behavioral dimorphism under early environmental constraints; bottom: mixed trajectories emerging at 20 min, as collective interactions begin to affect individual motion. (b) Temporal evolution of the average trajectory velocity during early expansion of the microcolony, reflecting the adaptation of individual activity. Group differences were assessed by one-way ANOVA followed by Tukey's HSD post hoc test for pairwise comparisons. Significance was set at $p < 0.05$. Different lowercase letters indicate statistically significant differences between groups ($p < 0.05$), whereas groups sharing the same letter are not significantly different. Data are presented as mean ± SD (or mean ± SEM). (c) Distribution of instantaneous bacterial speeds at selected time points. (d) Time-dependent changes in radius of gyration (Rg) of individual trajectories. (e) Distribution of anomalous diffusion exponents (α) for individual cells at various time points; inset highlights the high-α regime (superdiffusion).

values, implying that the cells adapted to the environment with increased motility (1st speed increase) (Fig. 3(c)). MSD and diffusion exponent α analysis showed that before ~ 15 min, most moving bacteria exhibited strong directionality with α values between ~ 1.8–1.9 and large Rg, consistent with long-distance exploration along relatively stable directions in free space (Figs. 3(d) and 3(e)). Over time, as the active medium began to be influenced by other cells, the bacteria made more random turns, while the directionality, α values, and Rg all began to decrease (Fig. S5 in the ESM). Such reduction of spatial coverage and superdiffusivity suggests an increase in cell–cell interactions.

2.3 Multistage dynamics under evolving pressures: transitions in organization and the interplay of cohesion and motility

As cell densities further increased, we were no longer able to track every motile cell using phase contrast microscopy. To resolve individual motility amidst increasing cell density throughout the subsequent microcolony evolution, we used a single-bacteria tracking method based on low-proportion fluorescent bacteria doping (ratios ranging from 1:50 to 1:20,000) (Movie S3 in the ESM). Control experiments confirmed that different doping ratios had no statistically significant effect on the measured kinematic parameters (Fig. S6 in the ESM).

Systematic analysis of thousands of single-cell trajectories revealed multi-stage phase transitions in individual dynamics (Fig. 4(a) and Fig. S7 in the ESM), reflecting the microcolony's journey through successive stages of organization, driven by the evolving nature of the fluid environment and collective interactions. After ~ 40 min (Movie S4 in the ESM), following initial environmental adaptation, the bacteria entered a phase characterized by rapid proliferation and increasing social interactions, which were driven by rising density and accumulating quorum sensing signals. Cells exhibited high motion efficiency with α maintained at ~ 1.8–1.9 (Fig. S8 in the ESM) and high directional persistence (sharp θ distribution). Average bacterial speed increased from ~ 37 to ~ 50 μm/s at ~ 80 min (2nd speed increase), with rapid expansion of motility range and average Rg reaching ~ 140 μm,

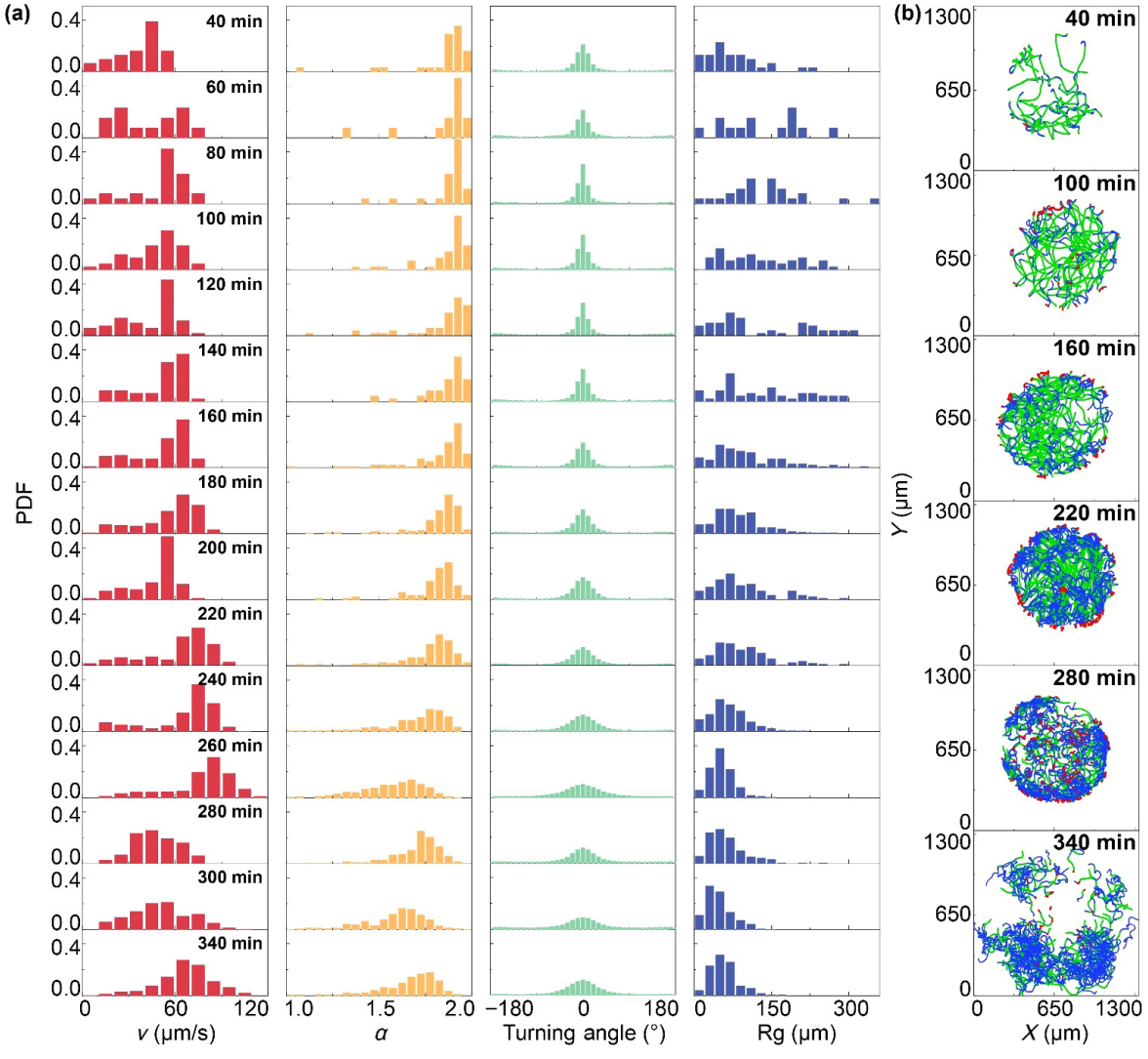

Figure 4 Multistage motility dynamics during the evolution of high-density bacterial colonies. (a) Time evolution of trajectory features: mean velocity (first column), mean diffusion exponent (second), turning angle (third), and mean gyration radius (fourth) per trajectory, quantifying the changes in individual cell dynamics throughout the microcolony's developmental stages. (b) Classification of trajectory segments (10 time-points long) into 3 motility states using the Deep-SEES algorithm. Red, motion restricted; blue, turning; and green, linear movement.

though with high variance. During ~ 80–120 min (Movie S5 in the ESM), as cell–cell encountering probabilities greatly increased, the average speed kept largely unchanged with slight decrease, but the Rg values began to decline. After ~ 160 min, as cell clustering and multilayer structures began to form, cohesive forces became more dominant in structuring the active medium. Bacterial motion remained relatively free (α maintained at ~ 1.8) (Movie S6 in the ESM) but started to be constrained by the collective (Rg decreased to ~ 100 μm). The average speed again increased, reaching ~ 57 μm/s at ~ 180 min and ~ 77 μm/s at ~ 260 min (3rd speed increase), with a broader distribution and slight Rg decrease. These may reflect dynamic differentiation of individuals under intensified cell-to-cell pressure: some bacteria, succumbing to cohesive forces, "gave up" to form relatively static networks; while some others, actively maintaining motility and "fighting against" such constraints, increased their speed to navigate the denser environment. Subsequently (~ 260–300 min) (Movie S7 in the ESM), increasing crowding, structural complexity, and "motile-static" partitioning led to an average speed decrease (~50 μm/s at ~280 min), motion range contraction (Rg dropped to ~60 μm), and broadened turning angle distributions, signifying stronger local and collective constraints. After ~ 300 min, as the microcolony started to expand, edge bacteria exhibited the 4th speed increase (average back to ~ 66 μm/s at ~ 340 min) due to nutrient availability and reduced confinement, while the ones in the microcolony center remained constrained in a stable dense network.

To further quantify motility states, we applied the Deep-SEES algorithm to classify trajectory segments (10 frames in length) into linear, turning, or constrained motion (Fig. S9 in the ESM). Results indicated that linear and turning segments, reflecting active, relatively free movement, were prevalent throughout the colony evolution, both spatially and temporally. In contrast, constrained segments showed spatiotemporal dependence, becoming significant only within the narrow microcolony edge or within the dense central networks late in evolution (Fig. 4(b) and Fig. S10 in the ESM). This implies that for much of the time, motile bacteria largely navigated the colony without severe restriction, suggesting that the fluid medium and collective interactions facilitate persistent motility. Taken the data above together, we can see that even in the highly crowded late stages, a large population of motile bacteria anomalously maintained superdiffusive (α > ~ 1.6) with high speed. This is a key finding, suggesting the emergence of unique mechanisms within dense bacterial collectives (potentially hydrodynamic, local ordering, or cellular adaptations), which enable effective navigation and resist strong dynamical arrest, thus maintaining significant internal "activity". These finding challenges direct analogies to passive glassy or jammed systems and points towards adaptive strategies in living active matter.

2.4 Bacteria-fluid coupling: the active fluid medium

To investigate the hydrodynamics induced by bacterial motility—the direct manifestation of the *Copula*—we introduced passive small oil-droplets (< 0.22 μm) as fluid nanotracers into the initial suspension (Movie S8 in the ESM). These surfactant-coated oil-nanotracers remained well-dispersed and floated near the surface, enabling simultaneous tracking with bacteria under phase-contrast microscopy (Fig. 5(a) and Fig. S11 in the ESM). We note that to ensure enough motile cells in the bacterial microcolony and prevent strong sticking of the oil-nanotracers to agar surface, a higher bacterial suspension was used and the initial cell count in bacterial droplet is ~ 6000, accelerating the microcolony expansion onset to ~ 220 min, about 50% faster than other colonies, but the overall evolutionary sequence remained comparable (Fig. S12 in the ESM).

The oil-nanodroplet dynamics clearly reflected the emergence of collective bacterial behavior and the establishment of an effective fluid transport network, which is the *Copula* in its dynamic, active form (Fig. 5(b)). Before ~ 30 min (early stage), limited cell activity resulted in sparse trackable nanodroplets exhibiting near-Brownian motion (α ~ 1) with near-uniform turning angle distribution. This is in sharp contrast with bacterial directionality. Average nanotracer speed increased from ~ 3 to ~8 μm/s (Fig. S13 in the ESM). During ~ 40–210 min (mid-stage), as bacterial density and collective motion increased, trackable nanodroplets increased significantly. Their dynamics transitioned to superdiffusion, driven by collective action. The directionality gradually strengthened in ~ 40–160 min. The average speed increased from ~ 9 μm/s to a peak of ~ 20–21 μm/s in ~ 160–210 min. Meanwhile, the average diffusion exponent α increased to ~ 1.2–1.3, albeit with significant spatiotemporal heterogeneity (Fig. S14 in the ESM). A subsequent decrease in trackable nanodroplets (~ 190–210 min) coincided with formation of static networks (probably because the imaging technique cannot distinguish trapped nanodroplets from dense bacteria), accompanied by a contraction in motility range and slight decrease in directionality. After ~ 220 min (late stage), while the microcolony expansion increased the active bacterial regions and the trackable droplets rebounded, most nanotracers did not spread outward with the bacteria. Their motility range continued to decrease, and their average speed dropped significantly (from ~ 20 μm/s pre-expansion to ~ 7–8 μm/s post-expansion), suggesting their confinement by the dense internal networks (Fig. S14 in the ESM). Interestingly, during this phase, directional persistence of the nanodroplets strengthened again, and the average diffusion exponent rose further to α ~ 1.5. This emergence of ordered flow despite network constraints is consistent with previous findings in larger, expanding colonies, underscoring a key mechanism: Dense bacterial interactions would self-coordinate, resulting in long-range hydrodynamic effects capable of driving ordered transport, establishing an "active fluid" state.

Further comparison using Lévy Walk (LW) fitting solidified the active-passive dynamical differentiation. While most bacterial trajectories (all stages) and many later-stage nanodroplet trajectories fit LW characteristics (Figs. S15 and S16 in the ESM), their parameters evolved differently. For bacteria, the step-length exponent μ increased (2.1 to 2.4) and the angle threshold θ_{max} increased (10° to 25°) with cell density, indicating suppressed long steps and reduced directionality (Fig. S17 in the ESM). Conversely, for mid- and late-stage nanodroplets, μ decreased (3.1 to 2.6) and θ_{max} decreased (65° to 45°), suggesting an increased probability of longer steps and enhanced directionality within the fluid field itself (Fig. 5(c) and Fig. S18 in the ESM), demonstrating the medium's transition to a more actively driven state. Despite these trends, crucial differences persisted: (1) The nanotracer average velocity remained much lower than bacteria (Fig. 5(d)); (2) the nanotracer superdiffusion ($\alpha \leq 1.5$) was consistently less efficient than bacterial superdiffusion (α > ~ 1.6) (Fig. 5(e)); (3) the nanotracer directionality was always weaker than bacteria's. These findings clearly show that the bacteria, as active agents, navigate the flow more efficiently, while the oil-nanotracers passively report the complex, collectively generated flow field. Consequently, the inter-

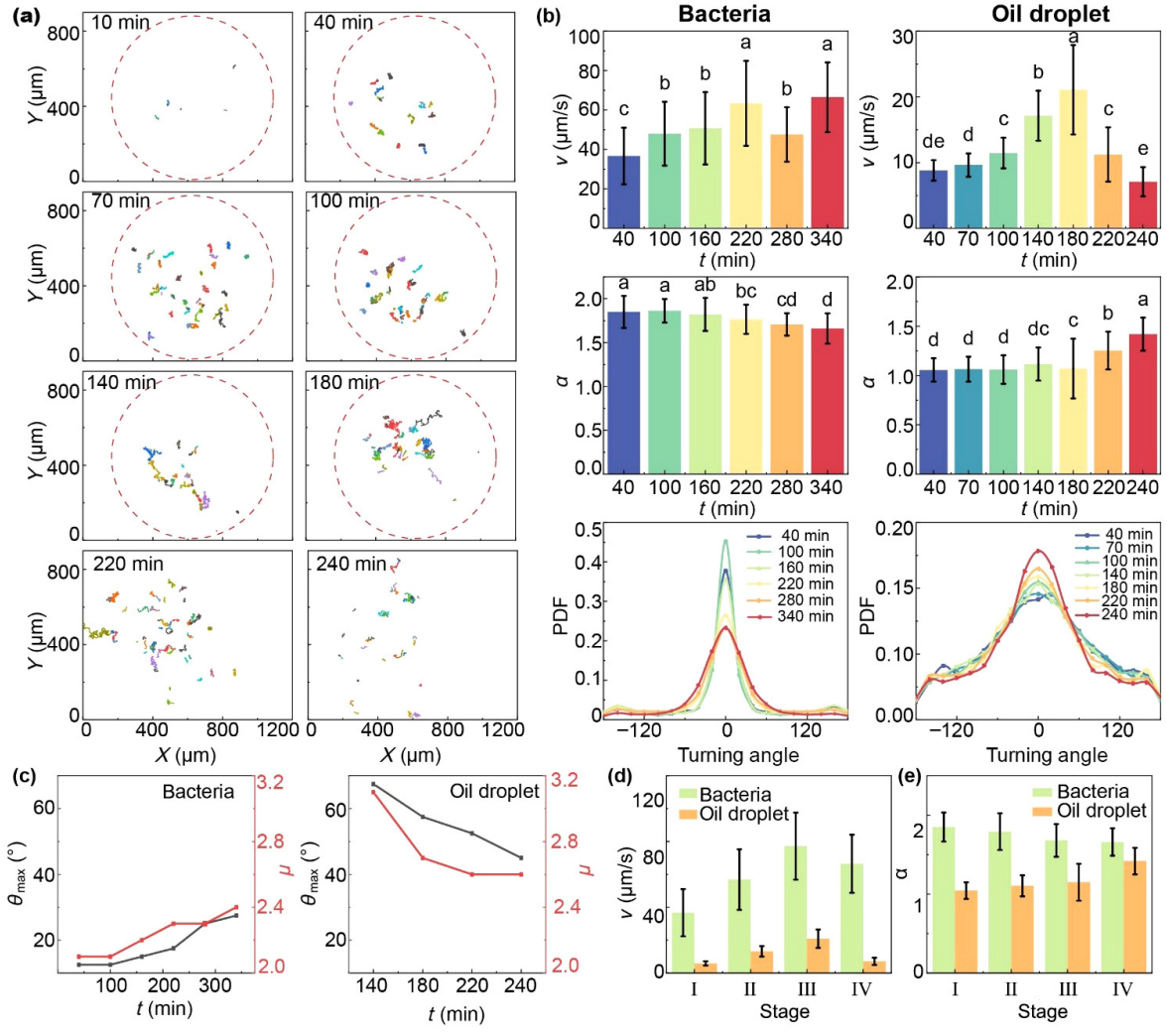

Figure 5 Coupling between bacterial motility and hydrodynamics during the microcolony development. (a) Trajectories of small oil-droplets at selected time-points reveal fluid motion induced by bacterial activity. (b) Temporal evolution of motility parameters for bacteria (active agents) and oil-nanodroplets (passive tracers), including speed (top row), anomalous diffusion exponent (middle row), and turning angle distribution (bottom row). (c) Time-dependent changes in the step length exponent (μ) and turning angle threshold (θ_max), obtained from Lévy walk fitting of bacterial and nanodroplet trajectories, respectively. Comparison of average speed (d) and superdiffusion exponent (e) between bacteria and nanodroplets at different colony development stages highlights differences between active agents and passive tracers.

bacterial fluid functions as an intermediary: being produced by the bacteria, it in turn influences the bacterial motion, thereby highlighting the interconnected co-evolution of bacterial motility and the active fluid environment.

3 Discussion

In this study, using a global, single-cell resolution, long-term observation platform, we provided a holistic view of the complete evolutionary picture of *Bacillus subtilis* microcolony. By tracking individual bacteria (the individual *Momente*) and passive fluid nanotracers (revealing the "active medium" or *Copula*) from the initial settlement of a few hundred cells to the formation of a dense, structured collective of several million (the *Entity* in its emergent form), we unveiled a multi-stage dynamic process driven by individual adaptive choices in response to multiple environmental, social, differentiation, and boundary pressures sequentially. These pressures can be viewed as successive manifestations of the *Copula*'s influence as the *Entity* evolves through different potencies, all ultimately rooted in the fundamental biological imperative of the bacteria to survive/thrive. In contrast to the philosophical inquiries of earlier centuries, where the individual-whole relationship and the nature of life's organizing principles were largely understood through theoretical speculation due to limited observational capabilities, our "whole-in-view" approach, without steady-state assumptions, offers direct, high-spatiotemporal resolution empirical evidence for these principles in a simple living system, revealing the intricate dynamics of early stages of collective life.

The earliest phase of microcolony development (< 15 min) is dominated by strong environmental pressure from the spread, ultra-thin liquid film and the intense interfacial effects. The observed behavioral bifurcation—where adjacent individuals in the central region adopt either near-linear traversal or large-radius circular motion—highlights a fascinating aspect of early adaptation [37, 38]. This "free" selection suggests that minute stochasticity or subtle variations in individual interactions with the interfaces are significantly amplified by the extreme physical constraints, leading to distinct, sustained movements. This brief window of extreme behavioral choice can be interpreted as the exploration of divergent strategies for persistence and expansion within a challenging initial

environment, driven by the survival imperative and amplified by the boundary conditions imposed by the early, constrained *Copula*.

As the cell density further increases, individuals face escalating social pressure from their neighbors and the emerging collective structure. This signifies a shift in the nature of the active medium, becoming dominated by cell–cell interactions and emergent forces that mediate competition and cooperation for resources and space. Global, long-term tracking reveals that single-cell dynamics do not change monotonically but undergo a series of multistage phase transitions, each marking an adaptation to a dominant pressure. These transitions can be seen as the *Entity* passing through different potencies of organization or the evolving *Copula*, as the bacteria collectively navigate the changing landscape of challenges and opportunities in their pursuit of survival and proliferation. The initial adaptation to environmental constraints sees the first speed increase (to ~ 37 μm/s), reflecting the individual asserting its motility as a means of exploring and exploiting the new setting. Subsequently, as social interactions intensify, a second speed increase (to ~ 50 μm/s) occurs, implying that early-to-moderate cell density and interactions might enhance motility efficiency, perhaps through collective drafting or optimized local flows, while individual cells still maintain highly efficient Lévy-walk-like exploration (α ~ 1.8–1.9). This period represents a transition from predominantly individual exploration to the nascent stages of coordinated group behavior.

The onset of differentiation pressure, as the microcolony develops dynamic structures like motile/static domains and interconnected networks, marks a crucial juncture. Individuals are now facing a "choice"—either assimilate into the relatively static structural elements or maintain motility within the increasingly complex and overcrowded environment. It is during this phase that we observe the most complex speed dynamics, including a 3rd significant speed increase (to > 60 μm/s) for motile individuals, potentially reflecting a subpopulation specializing in rapid movement or navigating newly formed channels, followed by a speed decrease as static domains become more extensive. This dynamic is an empirical manifestation of the tension between the principles of unifying and individuating within the actively constituting system, driven by the adaptive strategies employed by the bacteria. This period also marks the onset of a substantial decrease in superdiffusivity (α approaching ~ 1.6), suggesting increasingly stringent collective constraints imposed by the evolving active medium. Finally, as the microcolony surmounts boundary pressure and commences expansion, a 4th speed increase is observed at the leading edge, driven by nutrient availability and reduced confinement, enabling the pursuit of new territory. This entire sequence, a "micro-social history" of adaptation, underscores the remarkable plasticity of individual behavior in response to the evolving collective context and the dynamic *Copula* that governs their interactions, all due to the basic needs to survive and expand.

One interesting finding of this study is the anomalous persistence of significant superdiffusion (average α ~1.6) among motile bacteria even in the extremely crowded, late-stage of the microcolony. This observation challenges the common expectation from dense passive systems or many simple active particle models, which often predict a swift transition to subdiffusion ($\alpha < 1$) or a glassy state under such high densities [39, 40]. Instead of individuals simply "overcoming" a pre-existing jammed state, our findings suggest that the bacterial collective, as a micro-*Entity*, adaptively maintains a high level of internal "activity". The co-evolution of relatively static structural domains and a population of highly motile individuals appears to be an integral part of the self-organized state, demonstrating the *Entity* actively resisting a state of pure "inertness". This differentiation and sustained "activity" are likely crucial for maintaining material exchange, signal propagation, and responsiveness to environmental cues within the dense ensemble [41, 42], all vital for collective survival. Potential mechanisms enabling this "smooth navigation" through crowded environments could involve hydrodynamic interactions facilitating "slip" past neighbors, the formation of transient, locally ordered flow channels by collective motion, or intrinsic cellular properties such as shape, flexibility, and continuous metabolic energy input that actively resist complete dynamical arrest. Understanding this motility under high-density as a feature of an adaptively maintained active state, offers a biologically pertinent view on the *Entity*'s self-constitution in a non-equilibrium state.

The synchronous tracking of individual bacteria and single passive oil-nanodroplets provides direct insight into the co-evolution of bacterial motility and the induced fluid environment, revealing a clear active–passive dynamical differentiation and the dual role of the active fluid field as the *Copula*. The transition of oil-nanodroplet dynamics from early near-Brownian motion to later superdiffusion, accompanied by an enhanced directional persistence, demonstrates that bacterial collective self-organizes to generate long-range, active hydrodynamic effects with the potential to drive ordered macroscopic fluid transport. This emergent "active bath" is imperative for internal mixing, nutrient distribution, and signal propagation within the dense colony, thereby ensuring the collective survival. The quantitative disparity in superdiffusivity between active bacteria and the passive oil-nanodroplets, in conjunction with diverging LW characteristics, underscores that the emergent fluid field possesses its own spatiotemporal structure (e.g., local vortices, shear zones). The fluid field thus serves as the dynamic intermediary in spatiotemporal bacterial interactions, exerting feedbacks that shape bacterial behavior and the collective organization [43, 44]. It is the reciprocal action of individual *Momente* and the *Copula* that drives the self-constitution of the micro-*Entity*. Understanding this intricate, two-way coupling between individual activities and the collective flow, is paramount for accurately modeling and predicting the behavior of dense active matter systems.

4 Conclusions

In conclusion, by providing an unprecedented global view of microcolony evolution, we systematically unveil the multistage dynamics driven by individual adaptive choices under evolving pressures, interpreted here as a micro-*Entity* unfolding through successive potencies mediated by the "active medium" or *Copula*. Fueled by the fundamental biological imperative of survival and thriving, this process offers a compelling empirical illustration of how nature organizes itself, thereby bridging insights previously confined to philosophical speculation with rigorous scientific observation. We have captured early behavioral bifurcation under extreme physical constraint (the distinct potencies of motion), quantified the multi-phase dynamical transitions of single bacteria (adaptation to the evolving *Copula*), and discovered the key phenomenon of anomalous persistent superdiffusion at high density, challenging conventional views on dense active matter (the *Entity* actively resisting "inertness"). Our findings underscore the remarkable ability of bacterial collectives to adaptively maintain

internal "activity" rather than simply succumbing to physical jamming. Furthermore, by using coupled fluid tracing, we have elucidated the manner in which collective bacterial behavior drives ordered fluid transport. We have also clearly distinguished the dynamics of active drivers versus passive responders, revealing the fluid medium as the *Copula* that binds and organizes the system in service of the collective's drive to survive. These insights contribute to a more profound comprehension of microbial sociality, biofilm formation, and non-equilibrium active matter physics. Moreover, they establish a novel experimental paradigm for investigating the intricate journey from individual behavior to collective function in complex living systems. The observed dynamic structuring, far from simple gradients, reflects the true complexity and adaptive ingenuity of self-organization in living matter, providing a rich dataset for future theoretical and modeling endeavors aimed at capturing the essence of this biological *Natura naturans*.

5 Materials and methods

5.1 Bacterial species and culture conditions

In this study, the wild-type *Bacillus subtilis* strain 3610 was used as a model for investigating bacterial community evolution. This Gram-positive, rod-shaped bacterium (0.7 × 4 μm) readily forms colonies and exhibits typical swarming behavior. For fluorescent tracking, a 3610 derivative expressing mCherry and resistant to chloramphenicol was employed. Both strains were cultured overnight at 37 °C and 200 rpm in Luria-Bertani (LB) medium containing 1% tryptone, 0.5% yeast extract, and 0.5% NaCl. The culture medium for the fluorescent variant was supplemented with 25 μg/mL chloramphenicol and 1 mM isopropyl-β-D-thiogalactopyranoside (IPTG) to maintain selective pressure and induce fluorescent protein expression.

5.2 Large-area long-term high-resolution imaging

To observe the microcolony evolution from the lag phase to the expansion phase, a solid swarming medium was prepared, which contains 1% tryptone, 0.5% yeast extract, 0.5% NaCl, and 0.5% agar. After autoclaving, 1 mL of the medium was dispensed into 35 mm diameter plates and allowed to solidify at room temperature for 20 min. For inoculation, one end of a glass electrode was pulled into a fine tip (with a controlled inner diameter) and rendered hydrophobic by immersion in a coating solution of perfluorooctyltriethoxysilane and octadecyltrimethoxysilane for 12 h, followed by drying at 65 °C for 4 h. The tip was then cut to approximately 20 μm to enable injection of 20–50 nL of bacterial suspension (OD_{600} ≈ 0.4) onto the agar surface, forming an initial microcolony of 600–900 μm in diameter. After inoculation, plates were incubated at 30 °C and continuously imaged at 10 fps for 6 h using an Olympus CKX53 inverted microscope equipped with a 20× phase contrast objective and a DHYANA2100 sCMOS camera (TUCSEN), capturing the full dynamic process from the microcolony initiation to expansion.

5.3 Single-bacterium motion imaging at high density

To enable accurate tracking of individual bacteria under high-density conditions, the original solid swarming medium was supplemented with 1 mM IPTG and 1% anti-photobleaching agent. 4 mixtures of fluorescent and non-fluorescent bacteria were prepared at ratios of 1:50, 1:2000, 1:5000, and 1:20,000, respectively. Approximately 30 nL of each mixture was inoculated onto the agar surface. Fluorescence imaging was performed using a Nikon ECLIPSE Ti2 inverted microscope equipped with a Dragonfly high-speed spinning disk confocal system and a 10× objective lens, capturing images at 10 fps for single-cell trajectory analysis. Parallel samples with varying fluorescent labeling ratios were compared to ensure consistent motility characteristics under identical evolutionary timeframes. The agreement across multiple kinematic parameters confirmed that the tracking method did not significantly affect the observed motion behavior.

5.4 Flow field tracking using small oil-droplets

To investigate the influence of fluid flow on colony evolution, small oil-droplets were employed as nanotracers. A mixture of 1000 μL LB, 500 μL mineral oil, and 50 μL Tween 80 was prepared and vigorously vortexed to disperse the oil phase. The emulsion was then filtered through a 0.22 μm membrane to ensure that the resulting oil-droplet size was about 200 nm. A 1 mL bacterial suspension in the exponential growth phase (OD_{600} ≈ 0.4) was mixed with 50 μL of the prepared oil-droplet suspension by gentle pipetting. Approximately 30 nL of the mixture was injected onto the agar surface using the same glass electrode injection setup. The plate was immediately covered and incubated under controlled temperature and humidity conditions. The motion of both oil-nanodroplets and bacteria was recorded at 10 fps using an Olympus CKX53 inverted microscope equipped with a 20× phase contrast lens and a DHYANA2100 sCMOS camera (TUCSEN).

5.5 Image processing and data analysis

For the analysis of overall motion in high-density bacterial populations, PIV was performed using the open-source software MatPIV 1.6.1 developed by J. Kristian Sveen [45]. Continuous image sequences were processed with a large interrogation window of 64 × 64 pixels (approximately 14.4 μm × 14.4 μm), a small window of 32 × 32 pixels (approximately 7.2 μm × 7.2 μm), and a grid step of 3.6 μm. For the motion tracking of individual bacteria and oil-nanotracers in low-density conditions, the TrackMate plugin in ImageJ was used to detect and link single-particle trajectories. Subsequent analysis was performed using custom MATLAB scripts to calculate kinetic parameters such as velocity, directionality, and diffusion characteristics. Statistical modeling was applied based on relevant frameworks (e.g., Lévy walk). For trajectory classification, we employed the Deep-SEES algorithm [46], which integrates a variational autoencoder (VAE) with a long short-term memory (LSTM) network. This self-supervised learning approach extracts latent features from single-particle trajectories and effectively identifies and categorizes their dynamic states.

Electronic Supplementary Material: Supplementary material (PIV flow field measurements, single-cell trajectory tracking, motility parameter extraction, state classification with Deep-SEES, and Lévy walk analyses) is available in the online version of this article at https://doi.org/10.26599/NR.2026.94908449.

Data availability

All data needed to support the conclusions in the paper are presented in the manuscript and the Electronic Supplementary Material. Additional data related to this paper may be requested from the corresponding author upon request.

Acknowledgements

This work was supported by the National Natural Science Foundation of China (Nos. 22127807 and 91853105).

Declaration of competing interest

All the contributing authors report no conflict of interests in this work.

Author contribution statement

Y. Q. S.: Experimental design, investigation, data curation, writing manuscript. Q. R.: Investigation, data curation. Z. Y. Z.: Investigation. Y. Y. Z.: Data curation. Y. H.: Project administration, conceptualization, experimental design, data curation, writing manuscript. All the authors have approved the final manuscript.

Use of AI statement

During the preparation of this work, the authors used ChatGPT and Gemini Pro for lexical and syntactic suggestions and the readability of the language. After using these tools/services, the authors reviewed and edited the content as needed, and take full responsibility for the content of the publication.

References

[1] Grant, I. H. *Philosophies of Nature after Schelling*; Continuum International Publishing Group: London, 2008.
[2] Dear, P. *The Intelligibility of Nature: How Science Makes Sense of the World*; University of Chicago Press: Chicago, 2008.
[3] von Schelling, F. W. J. *Ideas for A Philosophy of Nature*; Cambridge University Press: Cambridge, 1988.
[4] Cohen, I. B. *The Birth of A New Physics*; WW Norton & Company: New York, 1985.
[5] Ling, H. J.; Mclvor, G. E.; van der Vaart, K.; Vaughan, R. T.; Thornton, A.; Ouellette, N. T. Costs and benefits of social relationships in the collective motion of bird flocks. *Nat. Ecol. Evol.* **2019**, *3*, 943–948.
[6] Shellard, A.; Mayor, R. Collective durotaxis along a self-generated stiffness gradient *in vivo*. *Nature* **2021**, *600*, 690–694.
[7] Lukeman, R.; Li, Y. X.; Edelstein-Keshet, L. Inferring individual rules from collective behavior. *Proc. Natl. Acad. Sci. USA* **2010**, *107*, 12576–12580.
[8] Kearns, D. B. A field guide to bacterial swarming motility. *Nat. Rev. Microbiol.* **2010**, *8*, 634–644.
[9] Bassler, B. L.; Losick, R. Bacterially speaking. *Cell* **2006**, *125*, 237–246.
[10] Drescher, K.; Dunkel, J.; Cisneros, L. H.; Ganguly, S.; Goldstein, R. E. Fluid dynamics and noise in bacterial cell-cell and cell-surface scattering. *Proc. Natl. Acad. Sci. USA* **2011**, *108*, 10940–10945.
[11] Koch, D. L.; Subramanian, G. Collective hydrodynamics of swimming microorganisms: Living fluids. *Annu. Rev. Fluid Mech.* **2011**, *43*, 637–659.
[12] Costerton, J. W.; Lewandowski, Z.; Caldwell, D. E.; Korber, D. R.; Lappin-Scott, H. M. Microbial biofilms. *Annu. Rev. Microbiol.* **1995**, *49*, 711–745.
[13] Copeland, M. F.; Weibel, D. B. Bacterial swarming: A model system for studying dynamic self-assembly. *Soft Matter* **2009**, *5*, 1174–1187.
[14] Flemming, H. C.; Wingender, J. The biofilm matrix. *Nat. Rev. Microbiol.* **2010**, *8*, 623–633.
[15] Bru, J. L.; Kasallis, S. J.; Zhuo, Q.; Høyland-Kroghsbo, N. M.; Siryaporn, A. Swarming of *P. aeruginosa*: Through the lens of biophysics. *Biophys. Rev.* **2023**, *4*, 031305.
[16] Hall-Stoodley, L.; Costerton, J. W.; Stoodley, P. Bacterial biofilms: From the natural environment to infectious diseases. *Nat. Rev. Microbiol.* **2004**, *2*, 95–108.
[17] Liu, J. T.; Prindle, A.; Humphries, J.; Gabalda-Sagarra, M.; Asally, M.; Lee, D. Y. D.; Ly, S.; Garcia-Ojalvo, J.; Süel, G. M. Metabolic co-dependence gives rise to collective oscillations within biofilms. *Nature* **2015**, *523*, 550–554.
[18] Prindle, A.; Liu, J. T.; Asally, M.; Ly, S.; Garcia-Ojalvo, J.; Süel, G. M. Ion channels enable electrical communication in bacterial communities. *Nature* **2015**, *527*, 59–63.
[19] Shapiro, J. A. Thinking about bacterial populations as multicellular organisms. *Annu. Rev. Microbiol.* **1998**, *52*, 81–104.
[20] Ramaswamy, S. The mechanics and statistics of active matter. *Annu. Rev. Condens. Matter Phys.* **2010**, *1*, 323–345.
[21] Nadell, C. D.; Xavier, J. B.; Foster, K. R. The sociobiology of biofilms. *FEMS Microbiol. Rev.* **2009**, *33*, 206–224.
[22] Flemming, H. C.; Wingender, J.; Szewzyk, U.; Steinberg, P.; Rice, S. A.; Kjelleberg, S. Biofilms: An emergent form of bacterial life. *Nat. Rev. Microbiol.* **2016**, *14*, 563–575.
[23] Lushi, E.; Wioland, H.; Goldstein, R. E. Fluid flows created by swimming bacteria drive self-organization in confined suspensions. *Proc. Natl. Acad. Sci. USA* **2014**, *111*, 9733–9738.
[24] Morales-Soto, N.; Anyan, M. E.; Mattingly, A. E.; Madukoma, C. S.; Harvey, C. W.; Alber, M.; Déziel, E.; Kearns, D. B.; Shrout, J. D. Preparation, imaging, and quantification of bacterial surface motility assays. *J. Vis. Exp.* **2015**, e52338.
[25] Wang, X. D.; Chen, S. S.; Bi, X. J.; Chen, N.; Yang, T.; Wang, L.; Maletskyi, Z.; Ratnaweera, H. Morphological image analysis of biofilm evolution with quantitative analysis in a moving bed biofilm reactor. *Sci. Total Environ.* **2023**, *856*, 159199.
[26] Karatan, E.; Watnick, P. Signals, regulatory networks, and materials that build and break bacterial biofilms. *Microbiol. Mol. Biol. Rev.* **2009**, *73*, 310–347.
[27] Serra, D. O.; Hengge, R. Bacterial multicellularity: The biology of *Escherichia coli* building large-scale biofilm communities. *Annu. Rev. Microbiol.* **2021**, *75*, 269–290.
[28] Jeckel, H.; Nosho, K.; Neuhaus, K.; Hastewell, A. D.; Skinner, D. J.; Saha, D.; Netter, N.; Paczia, N.; Dunkel, J.; Drescher, K. Simultaneous spatiotemporal transcriptomics and microscopy of *Bacillus subtilis* swarm development reveal cooperation across generations. *Nat. Microbiol.* **2023**, *8*, 2378–2391.
[29] Korshoj, L. E.; Kielian, T. Bacterial single-cell RNA sequencing captures biofilm transcriptional heterogeneity and differential responses to immune pressure. *Nat. Commun.* **2024**, *15*, 10184.
[30] Wensink, H. H.; Dunkel, J.; Heidenreich, S.; Drescher, K.; Goldstein, R. E.; Löwen, H.; Yeomans, J. M. Meso-scale turbulence in living fluids. *Proc. Natl. Acad. Sci. USA* **2012**, *109*, 14308–14313.
[31] Grauer, J.; Löwen, H.; Be'er, A.; Liebchen, B. Swarm hunting and cluster ejections in chemically communicating active mixtures. *Sci. Rep.* **2020**, *10*, 5594.
[32] Ning, L. H.; Lou, X.; Ma, Q. L.; Yang, Y. C.; Luo, N.; Chen, K.; Meng, F. L.; Zhou, X.; Yang, M. C.; Peng, Y. Hydrodynamics-induced long-range attraction between plates in bacterial suspensions. *Phys. Rev. Lett.* **2023**, *131*, 158301.
[33] Jeckel, H.; Jelli, E.; Hartmann, R.; Singh, P. K.; Mok, R.; Totz, J. F.; Vidakovic, L.; Eckhardt, B.; Dunkel, J.; Drescher, K. Learning the space-time phase diagram of bacterial swarm expansion. *Proc. Natl. Acad. Sci. USA* **2019**, *116*, 1489–1494.
[34] Sang, Y. Q.; Wen, X. D.; He, Y. Single-cell/nanoparticle trajectories reveal two-tier Lévy-like interactions across bacterial swarms. *View* **2022**, *3*, 20220047.
[35] Peñil Cobo, M.; Libro, S.; Marechal, N.; D'Entremont, D.; Peñil Cobo, D.; Berkmen, M. Visualizing bacterial colony morphologies using time-lapse imaging chamber MOCHA. *J. Bacteriol.* **2018**, *200*, e00413–17.
[36] Futo, M.; Široki, T.; Koska, S.; Čorak, N.; Tušar, A.; Domazet-Lošo,

M.; Domazet-Lošo, T. A novel time-lapse imaging method for studying developing bacterial biofilms. *Sci. Rep.* **2022**, *12*, 21120.
[37] Lauga, E.; DiLuzio, W. R.; Whitesides, G. M.; Stone, H. A. Swimming in circles: Motion of bacteria near solid boundaries. *Biophys. J.* **2006**, *90*, 400–412.
[38] Berke, A. P.; Turner, L.; Berg, H. C.; Lauga, E. Hydrodynamic attraction of swimming microorganisms by surfaces. *Phys. Rev. Lett.* **2008**, *101*, 038102.
[39] Lama, H.; Yamamoto, M. J.; Furuta, Y.; Shimaya, T.; Takeuchi, K. A. Emergence of bacterial glass. *PNAS Nexus* **2024**, *3*, pgae238.
[40] Sadhukhan, S.; Dey, S.; Karmakar, S.; Nandi, S. K. A perspective on active glassy dynamics in biological systems. *Eur. Phys. J. Spec. Top.* **2024**, *233*, 3193–3224.
[41] Ariel, G.; Be'er, A.; Reynolds, A. Chaotic model for Lévy walks in swarming bacteria. *Phys. Rev. Lett.* **2017**, *118*, 228102.
[42] Be'er, A.; Ariel, G. A statistical physics view of swarming bacteria. *Mov. Ecol.* **2019**, *7*, 9.
[43] Wu, X. L.; Libchaber, A. Particle diffusion in a quasi-two-dimensional bacterial bath. *Phys. Rev. Lett.* **2000**, *84*, 3017–3020.
[44] Feng, J. J.; Zhang, Z. X.; Wen, X. D.; Xue, J. F.; He, Y. Single nanoparticle tracking reveals efficient long-distance undercurrent transport in upper fluid of bacterial swarms. *iScience* **2019**, *22*, 123–132.
[45] Thielicke, W.; Stamhuis, E. J. PIVlab-towards user-friendly, affordable and accurate digital particle image velocimetry in MATLAB. *J. Open Res. Softw.* **2014**, *2*, e30.
[46] Zhang, Y. Y.; Ge, F.; Lin, X. J.; Xue, J. F.; Song, Y. X.; Xie, H.; He, Y. Extract latent features of single-particle trajectories with historical experience learning. *Biophys. J.* **2023**, *122*, 4451–4466.